

Fig. 11 Recall results for all tested methods over all categories.

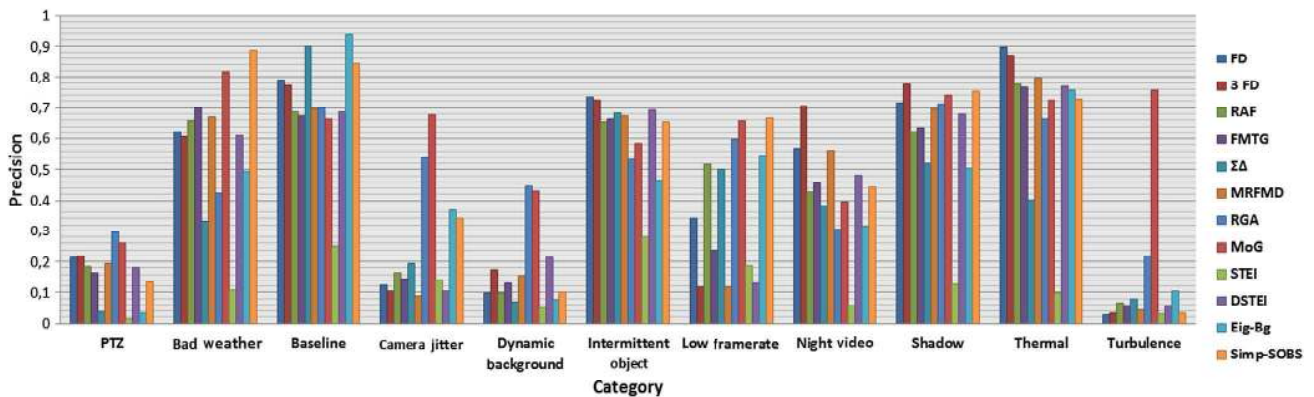


Fig. 12 Precision results for all tested methods over all categories.

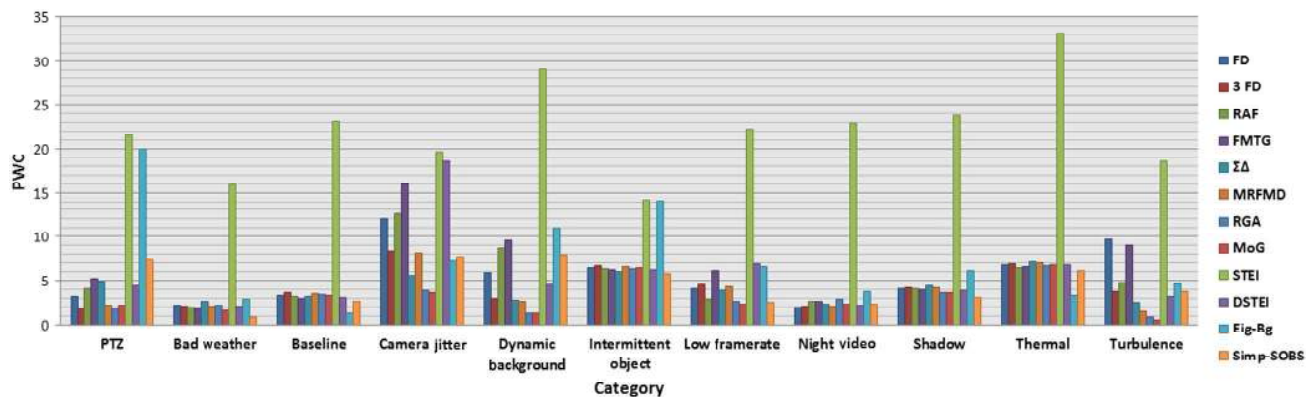


Fig. 13 PWC results for all tested methods over all categories.

video were eliminated, whereas the objects in motion were not well segmented. We note also that this method has a high precision in the case of “baseline” category, Fig. 12; however, results on this category, Fig. 15, show holes left in the segmented objects (high misses) which produce a low recall (Fig. 11 and Table 8), and this problem is owed to the initialization step based on temporal differencing.

The MRFMD method also yielded poor results and was similar to the $\Sigma\Delta$ method, with a high FNR and low recall (Figs. 11 and 17), due to its dependence on the

initialization step based on the temporal differencing method, leading to incompletely segmented moving objects (holes). Nevertheless, this method performed well by enhancing the image difference in terms of specificity (Fig. 16), and PWC (Fig. 13) has acceptable precision in the cases of “bad weather,” “shadow,” “night video,” and “thermal” (see Fig. 12 and Tables 5, 9–11).

In addition, this method is parametric because we had to define the values of the model energy ($\beta_s, \beta_p, \beta_f, \alpha$). Furthermore, the iterative conditional mode technique is

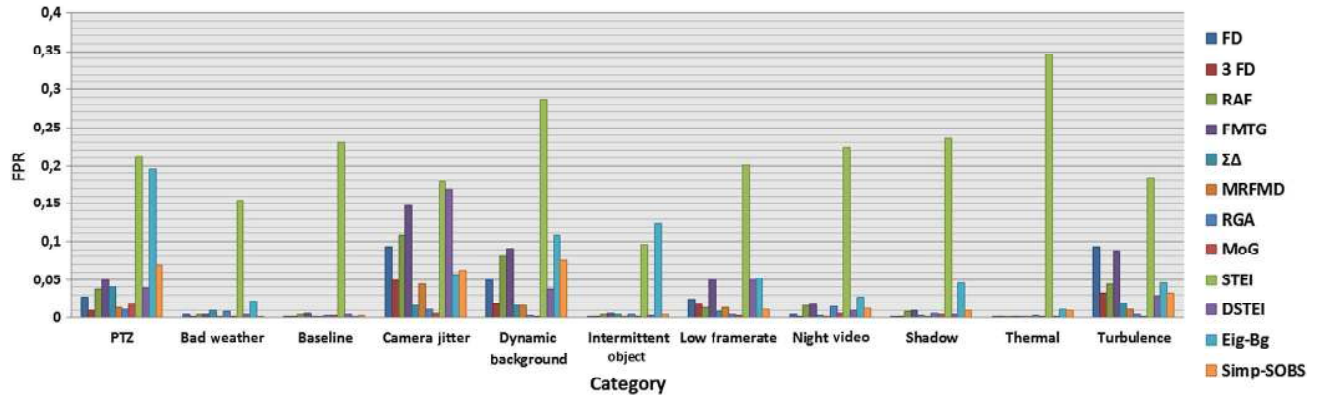


Fig. 14 FPR results for all tested methods over all categories.

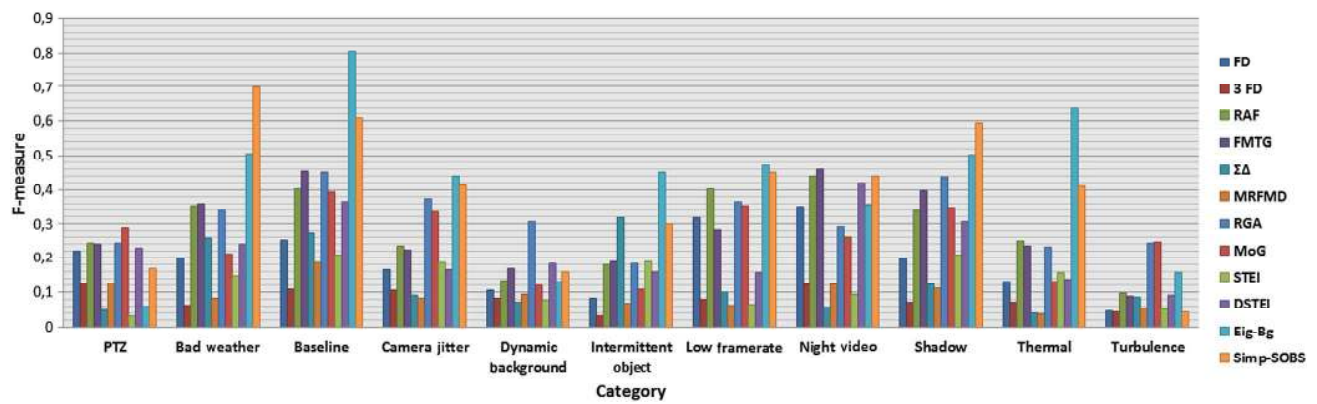


Fig. 15 F-measure results for all tested methods over all categories.

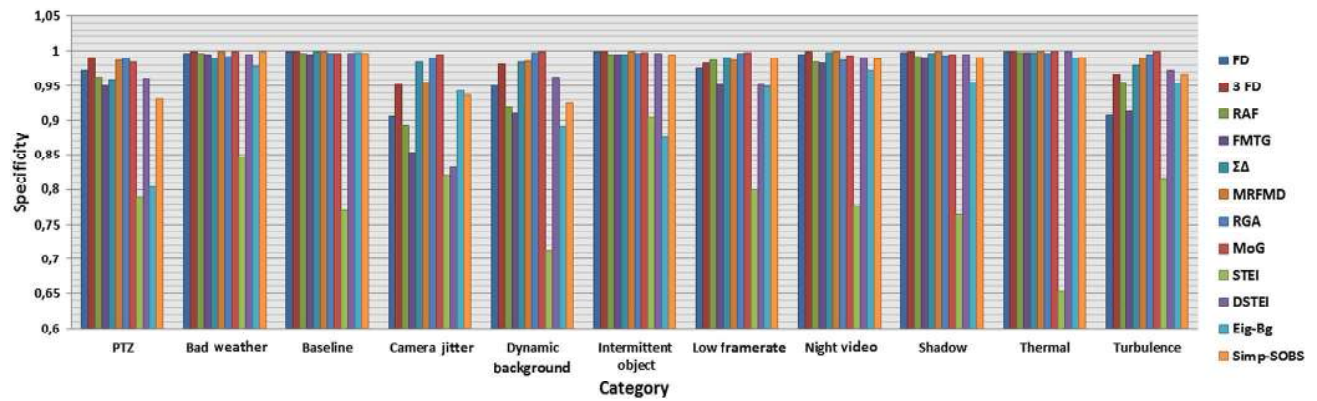


Fig. 16 Specificity results for all tested methods over all categories.

a suboptimal algorithm that may converge to local minima, but its computational time is considerably shorter than that of a stochastic relaxation scheme (i.e., simulated annealing).¹⁵⁹

As expected, the FD and 3-FD methods did not show good results, except for high precision, mainly because of the incomplete segmentation of the shape of moving objects, preserving only the edges. Moreover, these methods suffered from overlap of slow moving objects and poor detection of

objects far from the camera. To overcome the problem of incomplete segmentation, the threshold operation in the FD method is usually followed by morphological operations to link the edges of the moving objects. Then, regions and holes in the image are filled. Another solution is to combine FD methods with a background subtraction method.^{5,186} We also note that these methods demonstrate good detection of foreground pixels in night-time videos compared to background subtraction techniques, see Fig. 12 and Table 9,

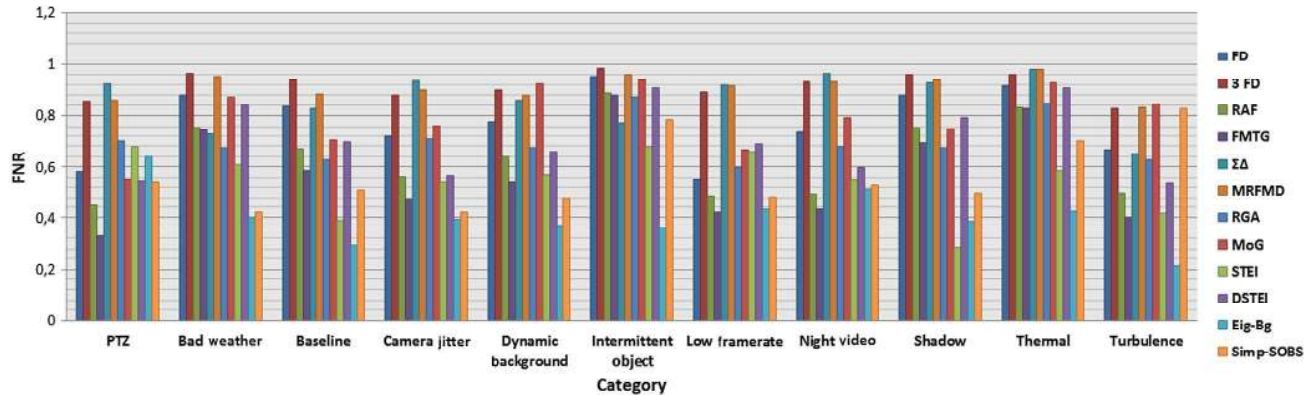


Fig. 17 FNR results for all tested methods over all categories.

owing to the change of light (vehicle or street light), which impairs the modeled background.

The FMTG method yielded acceptable results with observable low FNR (Fig. 17) and high recall (Fig. 11) for “PTZ,” “camera jitter,” “dynamic background,” “low frame rate,” “night video,” and “turbulence” categories (Tables 12 and 13). However, it was characterized by high FPR, caused by artificial tails due to an inappropriate value of α . Moreover, this method was conducive to strong background motion, as in the “dynamic background” category, Fig. 9.

As with FMTG, the RAF method yielded acceptable results. This result was expected because FMTG is based on a recursive operation of the RAF, i.e., Eq. (10). However, FMTG gave good detection results in bad weather conditions (see Figs. 12 and 15, Table 5) owing to the morphological temporal gradient filter, Eq. (15). Compared to FD and

3-FD, the RAF method outperforms them for almost all categories (except night videos) in terms of F -measure, FNR, and sensitivity, but with high FPR.

The fourth-best method according to the evaluation results (Table 3) was the Eig-Bg method, which yielded good detection results as well as silhouettes of objects. We noted that it had a high recall among all categories, Fig. 11 (except “low frame rate” category), and low FPR, Fig. 14. For “intermittent object” and “PTZ” categories, the Eig-Bg shows high FPR and PWC (Figs. 13, 14 and Tables 4, 14), and this is due to the absence of an update process in the original algorithm. Different techniques have been developed to resolve this problem; to this end we refer the reader to these Refs. 43, 69, 81, and 181. Remarkably, this method had a great precision and F -measure for the “baseline” category, which makes this method the ideal approach for easy and mild challenging

Table 4 Pixel-based evaluation of different motion detection methods applied to the “PTZ” category.

	Recall	Specificity	FPR	FNR	PWC	Precision	F -measure	RM_c
GMM	0.44955	0.98300	0.01700	0.55045	2.18306	0.26124	0.28955	3.57143
RGA	0.29935	0.98946	0.01054	0.70065	1.71521	0.29488	0.24364	3.71429
RAF	0.55135	0.96246	0.03754	0.44865	4.10254	0.18547	0.24236	4.42857
3-FD	0.14254	0.99055	0.00945	0.85746	1.74923	0.21983	0.12676	5.00000
FD	0.42000	0.97292	0.02708	0.58000	3.23362	0.21225	0.22099	5.28571
FMTG	0.67296	0.94991	0.05009	0.32704	5.22171	0.16603	0.24073	5.85714
DSTEI	0.45699	0.96035	0.03965	0.54301	4.42049	0.18210	0.22979	5.85714
MRFMD	0.13974	0.98662	0.01338	0.86026	2.14460	0.19404	0.12624	6.42857
Simp-SOBS	0.46153	0.93149	0.06851	0.53847	7.29140	0.13466	0.16815	7.42857
Eig-Bg	0.35897	0.80386	0.19614	0.64103	19.98432	0.03295	0.05791	9.71429
$\Sigma\Delta$	0.07621	0.95886	0.04114	0.92379	4.92846	0.03709	0.04640	9.85714
STEI	0.32390	0.78885	0.21115	0.67610	21.53317	0.01634	0.03047	10.85714

Table 5 Pixel-based evaluation of different motion detection methods applied to the “bad weather” category.

	Recall	Specificity	FPR	FNR	PWC	Precision	<i>F</i> -measure	<i>RM_c</i>
Simp-SOBS	0.58117	0.99862	0.00138	0.41883	0.87063	0.88652	0.69965	2.14286
GMM	0.12651	0.99966	0.00034	0.87349	1.67592	0.81834	0.21127	4.57143
FMTG	0.25595	0.99546	0.00454	0.74405	1.89175	0.70015	0.35741	5.00000
RAF	0.24383	0.99563	0.00437	0.75617	1.94594	0.65861	0.35216	5.57143
Eig-Bg	0.60037	0.97762	0.02238	0.39963	2.91987	0.49428	0.50623	6.57143
MRFMD	0.04452	0.99863	0.00137	0.95548	2.07388	0.67153	0.08175	6.85714
RGA	0.32721	0.99209	0.00791	0.67279	2.19833	0.42407	0.33892	7.14286
FD	0.12061	0.99620	0.00380	0.87939	2.18648	0.62279	0.19972	7.57143
DSTEI	0.15961	0.99509	0.00491	0.84039	2.11153	0.61012	0.24112	7.57143
3-FD	0.03300	0.99895	0.00105	0.96700	2.09177	0.60550	0.06235	7.71429
$\Sigma\Delta$	0.27268	0.98994	0.01006	0.72732	2.61408	0.33206	0.25832	8.14286
STEI	0.39261	0.84577	0.15423	0.60739	15.89976	0.10713	0.14777	9.14286

scenes. However, its results were strongly dependent on the images that form the eigenspace; the presence of moving objects in this space could alter the detection results. The execution time of this method depended on the number of eigenvectors. In our case, the execution time seemed acceptable for real-time application; however, memory requirements make it unsuitable for this type of application.

Methods based on Gaussian distributions showed better performance than other methods. The GMM method is characterized by its very high precision and high *F*₁-score in difficult challenging categories (“bad weather, dynamic background, camera jitter, low frame rate, shadow, and turbulence”), and has low PWCs and low FPR in all categories; this is due to the number of *K* Gaussians used to model the

Table 6 Pixel-based evaluation of different motion detection methods applied to the “camera jitter” category.

	Recall	Specificity	FPR	FNR	PWC	Precision	<i>F</i> -measure	<i>RM_c</i>
Eig-Bg	0.6076	0.9421	0.0579	0.3924	7.1837	0.3663	0.4391	3.1429
RGA	0.2905	0.9894	0.0106	0.7095	3.8901	0.5399	0.3741	3.5714
GMM	0.2374	0.9944	0.0056	0.7626	3.6016	0.6779	0.3344	3.7143
Simp-SOBS	0.5808	0.9373	0.0627	0.4192	7.7127	0.3411	0.4147	4.1429
RAF	0.4378	0.8926	0.1074	0.5622	12.6178	0.1664	0.2351	6.8571
FMTG	0.5246	0.8533	0.1467	0.4754	16.0025	0.1457	0.2236	7.0000
$\Sigma\Delta$	0.0637	0.9837	0.0163	0.9363	5.5428	0.1953	0.0898	7.0000
FD	0.2809	0.9061	0.0939	0.7191	12.0018	0.1227	0.1668	8.1429
3-FD	0.1188	0.9513	0.0487	0.8812	8.4001	0.1040	0.1065	8.2857
STEI	0.4609	0.8205	0.1795	0.5391	19.6615	0.1436	0.1872	8.4286
MRFMD	0.0987	0.9554	0.0446	0.9013	8.1616	0.0888	0.0824	8.5714
DSTEI	0.4354	0.8314	0.1686	0.5646	18.5179	0.1041	0.1648	9.1429

dynamic backgrounds. Notably, the RGA method outperforms the MoG method (Table 3), with higher recall (Fig. 11), low FNR values (Fig. 17), and higher *F*-measure (Fig. 15) in almost all categories. This is owed to the large number of parameters required to set for the MoG algorithm (K, α, T, D, σ), which differ with the challenging conditions

presented by a video (day/night, indoor/outdoor, complex/simple background, with/without noise). Thus, in some cases, the RGA method seemed to be sufficient. Moreover, its computational complexity was lower than that of the MoG method, as was found by Piccardi⁴ and Benetech et al.⁹⁷

Table 7 Pixel-based evaluation of different motion detection methods applied to the “dynamic background” category.

	Recall	Specificity	FPR	FNR	PWC	Precision	<i>F</i> -measure	RM_c
RGA	0.32604	0.99739	0.00261	0.67396	1.25771	0.44585	0.30555	3.00000
DSTEI	0.34040	0.96264	0.03736	0.65960	4.53876	0.21356	0.18193	5.00000
GMM	0.07816	0.99884	0.00116	0.92184	1.28203	0.43209	0.11900	5.28571
Simp-SOBS	0.52337	0.92515	0.07485	0.47663	7.89821	0.10130	0.16129	5.57143
MRFMD	0.11941	0.98458	0.01542	0.88059	2.65240	0.15423	0.09444	6.14286
FMTG	0.46085	0.90959	0.09041	0.53915	9.53249	0.12996	0.16795	6.42857
RAF	0.35967	0.91939	0.08061	0.64033	8.73891	0.09714	0.13346	7.14286
3-FD	0.09905	0.98135	0.01865	0.90095	2.95550	0.17437	0.08254	7.28571
Eig-Bg	0.62761	0.89217	0.10783	0.37239	11.02858	0.07684	0.13219	7.28571
$\Sigma\Delta$	0.13895	0.98350	0.01650	0.86105	2.75199	0.07037	0.07060	7.57143
FD	0.22397	0.95006	0.04994	0.77603	5.86099	0.09671	0.10502	7.71429
STEI	0.42841	0.71230	0.28770	0.57159	29.06152	0.05091	0.07804	9.57143

Table 8 Pixel-based evaluation of different motion detection methods applied to the “baseline” category.

	Recall	Specificity	FPR	FNR	PWC	Precision	<i>F</i> -measure	RM_c
Eig-Bg	0.70521	0.99832	0.00168	0.29479	1.32715	0.93552	0.80366	2.14286
Simp-SOBS	0.48942	0.99649	0.00351	0.51058	2.63660	0.84190	0.60852	3.85714
$\Sigma\Delta$	0.17359	0.99946	0.00054	0.82641	3.23513	0.90046	0.27642	5.42857
RGA	0.37160	0.99672	0.00328	0.62840	3.39816	0.69864	0.44997	5.85714
FMTG	0.41467	0.99483	0.00517	0.58533	3.00519	0.67255	0.45341	6.57143
FD	0.16392	0.99883	0.00117	0.83608	3.35138	0.79205	0.25216	6.71429
RAF	0.33089	0.99618	0.00382	0.66911	3.21227	0.68705	0.40236	7.14286
DSTEI	0.30211	0.99629	0.00371	0.69789	3.09809	0.68536	0.36369	7.42857
3-FD	0.06106	0.99947	0.00053	0.93894	3.61961	0.77192	0.10796	7.71429
GMM	0.29563	0.99640	0.00360	0.70437	3.30918	0.66375	0.39360	8.00000
MRFMD	0.11522	0.99872	0.00128	0.88478	3.51801	0.69588	0.18603	8.28571
STEI	0.60964	0.76918	0.23082	0.39036	23.14295	0.25211	0.20983	8.85714

Finally, Simp-SOBS showed the best results of all the methods, with high precision, recall, and *F*-measure, owing to the use of the HSV color space and the condition on the *V* value component that significantly reduced object shadows. Furthermore, we note from Table 15 that the results of this

method in challenging categories (“bad weather,” “low frame rate,” and “shadow”) were as good as those in simple categories (“baseline”). From the previous results, we can note that the most challenging categories for this method are: the “turbulence” category characterized by low precision

Table 9 Pixel-based evaluation of different motion detection methods applied to the “night video” category.

	Recall	Specificity	FPR	FNR	PWC	Precision	<i>F</i> -measure	<i>RM_c</i>
FD	0.26524	0.99547	0.00453	0.73476	2.01185	0.56769	0.35088	4.71429
DSTEI	0.40097	0.99043	0.00957	0.59903	2.24922	0.48116	0.42043	5.14286
3-FD	0.06949	0.99921	0.00079	0.93051	2.03676	0.70609	0.12229	5.28571
FMTG	0.56808	0.98238	0.01762	0.43192	2.63505	0.45533	0.46018	5.28571
Simp-SOBS	0.47254	0.98834	0.01166	0.52746	2.29129	0.44207	0.43995	5.28571
MRFMD	0.07002	0.99876	0.00124	0.92998	2.07952	0.56291	0.12237	5.57143
RAF	0.50793	0.98401	0.01599	0.49207	2.63158	0.42673	0.43843	5.71429
GMM	0.20595	0.99388	0.00612	0.79405	2.26189	0.39635	0.26142	7.00000
Eig-Bg	0.48550	0.97250	0.02750	0.51450	3.77828	0.31558	0.35541	7.71429
$\Sigma\Delta$	0.03625	0.99749	0.00251	0.96375	2.27967	0.38100	0.05685	8.14286
RGA	0.32350	0.98592	0.01408	0.67650	2.84418	0.30709	0.29126	8.28571
STEI	0.45413	0.77635	0.22365	0.54587	22.85890	0.05566	0.09322	9.85714

Table 10 Pixel-based evaluation of different motion detection methods applied to the “shadow” category.

	Recall	Specificity	FPR	FNR	PWC	Precision	<i>F</i> -measure	<i>RM_c</i>
Simp-SOBS	0.50198	0.99044	0.00956	0.49802	3.07260	0.75207	0.59353	4.28571
RGA	0.32784	0.99372	0.00628	0.67216	3.61823	0.71265	0.43611	4.57143
GMM	0.24914	0.99518	0.00482	0.75086	3.61844	0.74109	0.34635	5.00000
FD	0.11852	0.99764	0.00236	0.88148	4.08282	0.71392	0.19762	6.14286
DSTEI	0.20761	0.99541	0.00459	0.79239	3.92670	0.67913	0.30582	6.28571
FMTG	0.30569	0.99083	0.00917	0.69431	3.94654	0.63377	0.39529	6.42857
3-FD	0.03776	0.99962	0.00038	0.96224	4.24996	0.77620	0.07113	6.85714
Eig-Bg	0.61292	0.95488	0.04512	0.38708	6.08321	0.50480	0.50255	7.14286
MRFMD	0.06100	0.99894	0.00106	0.93900	4.24903	0.69451	0.11048	7.28571
RAF	0.24641	0.99171	0.00829	0.75359	4.09855	0.62128	0.33949	7.42857
$\Sigma\Delta$	0.07324	0.99648	0.00352	0.92676	4.39514	0.51865	0.12251	8.28571
STEI	0.71537	0.76417	0.23583	0.28463	23.76070	0.12635	0.20898	8.28571

(Fig. 12) and high FNR (Fig. 17), and the “PTZ” category characterized by high PWC (Fig. 13) and high FPR (Fig. 14).

Figure 18 shows the frame rate (execution time) of each method, applied on “PETS2006” video from the “baseline”

category, with a resolution of 720×576 . Tests were carried on Intel I7 2.3 GHz with 16 GB RAM, and parts of the code were nonvectorized. This figure shows that the fastest methods were DF, 3-FD, RAF, and FMTG because of their

Table 11 Pixel-based evaluation of different motion detection methods applied to the “thermal” category.

	Recall	Specificity	FPR	FNR	PWC	Precision	F-measure	RM_c
Eig-Bg	0.57527	0.98983	0.01017	0.42473	3.34477	0.75660	0.63940	4.71429
RAF	0.16894	0.99785	0.00215	0.83106	6.46159	0.77678	0.24840	4.85714
FD	0.08293	0.99952	0.00048	0.91707	6.76412	0.89736	0.13254	5.28571
FMTG	0.17280	0.99771	0.00229	0.82720	6.53223	0.76712	0.23493	5.42857
Simp-SOBS	0.30052	0.99103	0.00897	0.69948	6.14208	0.72833	0.40935	5.42857
DSTEI	0.09116	0.99884	0.00116	0.90884	6.80556	0.77026	0.13743	6.00000
3-FD	0.03946	0.99975	0.00025	0.96054	6.90147	0.87329	0.06998	6.42857
RGA	0.14817	0.99652	0.00348	0.85183	6.69029	0.66375	0.23215	7.14286
MRFMD	0.01977	0.99979	0.00021	0.98023	6.97932	0.79833	0.03642	7.28571
GMM	0.07448	0.99857	0.00143	0.92552	6.79791	0.72397	0.13242	7.57143
STEI	0.41382	0.65387	0.34613	0.58618	33.18293	0.09735	0.15688	8.28571
$\Sigma\Delta$	0.02021	0.99792	0.00208	0.97979	7.12201	0.40127	0.03848	9.57143

Table 12 Pixel-based evaluation of different motion detection methods applied to the “low frame rate” category.

	Recall	Specificity	FPR	FNR	PWC	Precision	F-measure	RM_c
Simp-SOBS	0.51954	0.98959	0.01041	0.48046	2.56486	0.66767	0.44959	2.71429
RGA	0.40264	0.99610	0.00390	0.59736	2.58883	0.59523	0.36304	3.71429
GMM	0.33327	0.99736	0.00264	0.66673	2.31369	0.65832	0.35273	3.71429
RAF	0.51335	0.98607	0.01393	0.48665	2.90861	0.51617	0.40144	4.57143
Eig-Bg	0.56639	0.94749	0.05251	0.43361	6.54513	0.54566	0.46997	5.85714
FD	0.45044	0.97505	0.02495	0.54956	4.09714	0.34237	0.31730	6.42857
FMTG	0.57796	0.95039	0.04961	0.42204	6.06386	0.23980	0.28403	6.57143
$\Sigma\Delta$	0.08207	0.99134	0.00866	0.91793	3.90652	0.50163	0.10016	7.14286
MRFMD	0.08464	0.98657	0.01343	0.91536	4.31021	0.11816	0.06137	8.85714
3-FD	0.10544	0.98281	0.01719	0.89456	4.58337	0.11600	0.08011	9.14286
DSTEI	0.31088	0.95063	0.04937	0.68912	6.88456	0.13012	0.15748	9.28571
STEI	0.34130	0.79972	0.20028	0.65870	22.17830	0.18730	0.06510	10.00000

simplicity. Eig-Bg shows also a good execution time, and this is interpreted by the use of a subset of singular values and vectors, which overcomes the long time required to compute the N eigenvectors using eigendecomposition. $\Sigma\Delta$ has a

slow frame rate owing to the postprocessing step required to eliminate the ghost effect. The slowest methods were MoG, STEI, and DSTEI; MOG is slow because of the computing complexity linked to the use of K Gaussian distributions,

Table 13 Pixel-based evaluation of different motion detection methods applied to the “turbulence” category.

	Recall	Specificity	FPR	FNR	PWC	Precision	F-measure	RM_c
RGA	0.37053	0.99522	0.00478	0.62947	0.89475	0.22000	0.24396	3.42857
GMM	0.15444	0.99975	0.00025	0.84556	0.46990	0.75562	0.24731	4.14286
Eig-Bg	0.78752	0.95435	0.04565	0.21248	4.71277	0.10395	0.15637	4.71429
Simp-SOBS	0.78287	0.95072	0.04928	0.21713	5.07985	0.11308	0.16392	5.28571
DSTEI	0.46520	0.97167	0.02833	0.53480	3.17950	0.05695	0.09098	5.71429
$\Sigma\Delta$	0.34950	0.97966	0.02034	0.65050	2.48953	0.07998	0.08646	5.85714
RAF	0.50183	0.95535	0.04465	0.49817	4.79166	0.06753	0.09773	6.14286
MRFMD	0.16698	0.98938	0.01062	0.83302	1.56510	0.04329	0.05261	7.00000
FMTG	0.59875	0.91203	0.08797	0.40125	9.05480	0.05586	0.08904	7.28571
3-FD	0.17101	0.96715	0.03285	0.82899	3.76600	0.03516	0.04327	8.57143
STEI	0.58499	0.81651	0.18349	0.41501	18.58043	0.03174	0.05193	9.28571
FD	0.33346	0.90664	0.09336	0.66654	9.71757	0.02896	0.04452	10.57143

Table 14 Pixel-based evaluation of different motion detection methods applied to the “intermittent object” category.

	Recall	Specificity	FPR	FNR	PWC	Precision	F-measure	RM_c
$\Sigma\Delta$	0.22742	0.99530	0.00470	0.77258	6.00318	0.68200	0.31732	4.28571
Simp-SOBS	0.21610	0.99506	0.00494	0.78390	5.81846	0.65376	0.30207	5.42857
DSTEI	0.09327	0.99691	0.00309	0.90673	6.23954	0.69406	0.15943	5.85714
RGA	0.12612	0.99609	0.00391	0.87388	6.33705	0.53360	0.18253	6.28571
FD	0.04566	0.99873	0.00127	0.95434	6.43023	0.73456	0.08313	6.42857
FMTG	0.11714	0.99452	0.00548	0.88286	6.18409	0.66480	0.19018	6.42857
RAF	0.10976	0.99541	0.00459	0.89024	6.31262	0.65421	0.18066	6.71429
Eig-Bg	0.63616	0.87557	0.12443	0.36384	14.03169	0.46714	0.45021	7.00000
3-FD	0.01516	0.99954	0.00046	0.98484	6.62883	0.72605	0.02929	7.14286
MRFMD	0.03628	0.99878	0.00122	0.96372	6.57922	0.67419	0.06807	7.28571
GMM	0.06211	0.99820	0.00180	0.93789	6.42132	0.58364	0.10818	7.28571
STEI	0.32070	0.90380	0.09620	0.67930	14.15520	0.27958	0.18753	7.85714

Table 15 Top three methods for all categories based on the average RC.

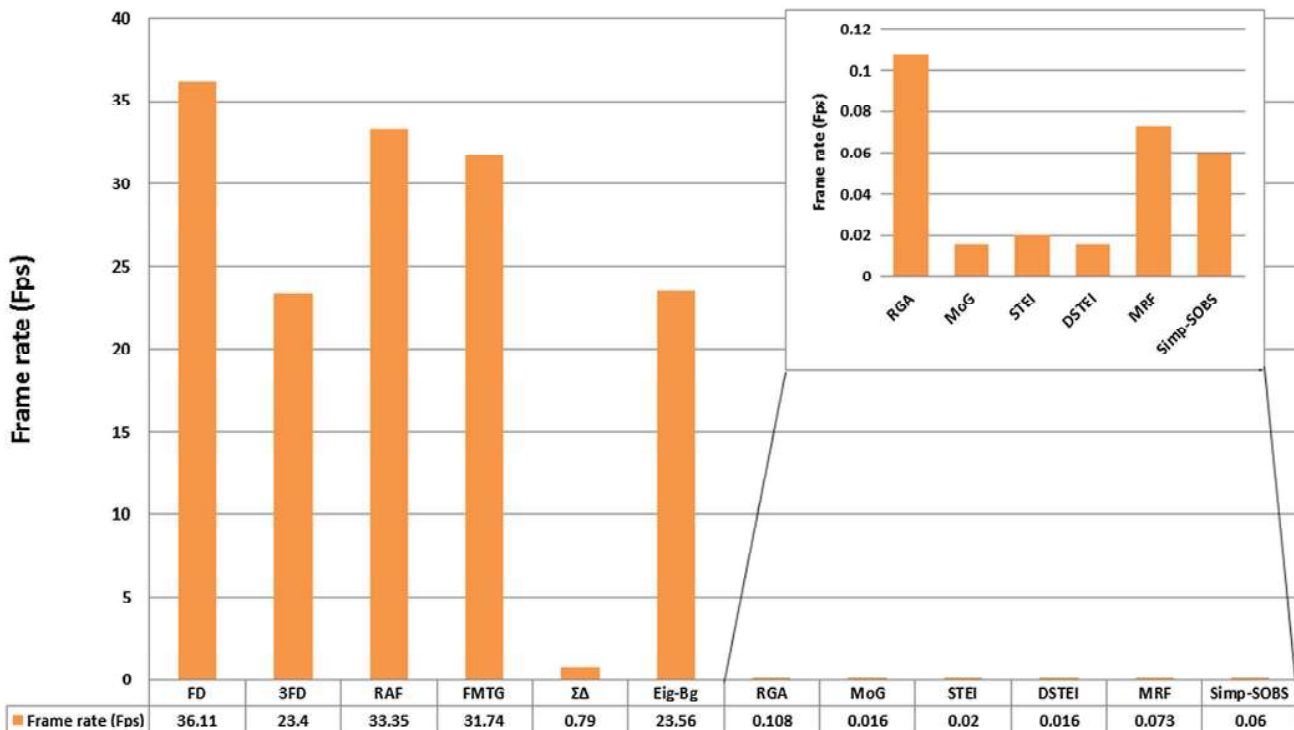
	First	Second	Third
PTZ	MoG	RGA	RAF
Bad weather	Simp-SOBS	MoG	FMTG
Baseline	Eig-Bg	Simp-SOBS	$\Sigma\Delta$
Camera jitter	Eig-Bg	RGA	MoG
Dynamic background	RGA	DSTEI	MoG
Intermittent object motion	$\Sigma\Delta$	Simp-SOBS	DSTEI
Low frame rate	Simp-SOBS	RGA	MoG
Night video	FD	3-FD	DSTEI
Shadow	Simp-SOBS	RGA	MoG
Thermal	Eig-Bg	RAF	FD
Turbulence	RGA	MoG	Eig-Bg

the time required to update their parameters, and to order them; and the slowness of STEI and DSTEI is more closely related to the time needed to compute the histogram from the spatio-temporal window. MRF, Simp-SOBS, and RGA also had long execution times, but they were not as slow as the previous methods.

6 Conclusion

In this paper, we review and compare motion detection methods using one of the most recent, complete, and challenging datasets: CDnet2012 and CDnet2014. Detailed pixel evaluation was performed using different metrics to enable a user to determine the appropriate method for his or her needs.

From the results reported, we can conclude that there is no ideal method for all situations; each method performs well in some cases and fails in others. However, it is worth mentioning here that methods based on FDs are not really designed to detect a complete silhouette of the moving object and thus are underrated here; they aim to detect motion and typically must be combined with other methods to achieve full segmentation. If we had to choose two methods based on the different challenging categories, they would be the Simp-SOBS²⁴ and the RGA¹⁴ methods; the former for the “bad weather,” “baseline,” “intermittent object motion,” “low frame rate,” “night video,” “shadow,” and “thermal” categories, and the latter for the “PTZ,” “camera jitter,” “dynamic background,” and “turbulence” categories. This choice is justified by the high ranks of the methods for nearly all categories based on the average RC as well as their acceptable execution times. The good performance of Simp-SOBS can be explained by the simple but powerful competitive learning used in SOM with an appropriate HSV color space that separates chromaticity from brightness information. The surprising results of RGA are linked to its low complexity with only a few parameters to adjust (e.g., compared to MoG¹⁵) that was sufficient for most areas of the images tested (only small image portions would have required more complex methods such as MoG), because the whole image background is not always dynamic except for the bad weather condition or

**Fig. 18** Computational time for each method (presented in frames per second).

maritime applications, where we found that the MoG is superior to the RGA in the tested categories). In the future, we will test other methods in order to expand the scope of this study and provide users with a complete benchmark of motion detection methods.

References

1. I. S. Kim et al., "Intelligent visual surveillance—a survey," *Int. J. Control. Autom. Syst.* **8**(5), 926–939 (2010).
2. M. Paul, S. M. Haque, and S. Chakraborty, "Human detection in surveillance videos and its applications—a review," *EURASIP J. Adv. Signal Process.* **2013**(1), 176 (2013).
3. W. Hu et al., "A survey on visual surveillance of object motion and behaviors," *IEEE Trans. Syst. Man Cybern. Part C* **34**(3), 334–352 (2004).
4. M. Piccardi, "Background subtraction techniques: a review," in *2004 IEEE Int. Conf. on Systems, Man and Cybernetics*, Vol. 4, pp. 3099–3104 (2004).
5. D. A. Migliore, M. Matteucci, and M. Naccari, "A revaluation of frame difference in fast and robust motion detection," in *Proc. of the 4th ACM Int. Workshop on Video Surveillance and Sensor Networks*, pp. 215–218 (2006).
6. S. Yalamanchili, W. N. Martin, and J. K. Aggarwal, "Extraction of moving object descriptions via differencing," *Comput. Graph. Image Process.* **18**(2), 188–201 (1982).
7. R. Jain, W. Martin, and J. Aggarwal, "Segmentation through the detection of changes due to motion," *Comput. Graph. Image Process.* **11**(1), 13–34 (1979).
8. B. D. Lucas and T. Kanade, "An iterative image registration technique with an application to stereo vision," in *Proc. 7th Int. Joint Conf. Artificial Intelligence*, Morgan Kaufmann Publishers Inc., San Francisco, California, pp. 674–679 (1981).
9. B. K. Horn and B. G. Schunck, "Determining optical flow: a retrospective," *Artif. Intell.* **59**(1–2), 81–87 (1993).
10. T. Bouwmans, "Recent advanced statistical background modeling for foreground detection—a systematic survey," *Recent Pat. Comput. Sci.* **4**(3), 147–176 (2011).
11. W.-X. Kang, W.-Z. Lai, and X.-B. Meng, "An adaptive background reconstruction algorithm based on inertial filtering," *Optoelectron. Lett.* **5**(6), 468–471 (2009).
12. S. Jiang and Y. Zhao, "Background extraction algorithm base on Partition Weighted Histogram," in *3rd IEEE Int. Conf. on Network Infrastructure and Digital Content (IC-NIDC 2012)*, pp. 433–437 (2012).
13. J. Zheng et al., "Extracting roadway background image: mode-based approach," *Transp. Res. Rec.* **1944**, 82–88 (2006).
14. C. R. Wren et al., "Pfinder: real-time tracking of the human body," *IEEE Trans. Pattern Anal. Mach. Intell.* **19**(7), 780–785 (1997).
15. C. Stauffer and W. E. L. Grimson, "Adaptive background mixture models for real-time tracking," in *IEEE Computer Society Conf. on Computer Vision and Pattern Recognition*, pp. 246–252 (1999).
16. A. Elgammal, D. Harwood, and L. Davis, "Non-parametric model for background subtraction," in *European Conf. on Computer Vision*, pp. 751–767 (2000).
17. F. El Baf, T. Bouwmans, and B. Vachon, "Type-2 fuzzy mixture of Gaussians model: application to background modeling," in *Int. Symp. on Visual Computing*, pp. 772–781 (2008).
18. M. H. Sigari, N. Mozayani, and H. Pourreza, "Fuzzy running average and fuzzy background subtraction: concepts and application," *Int. J. Comput. Sci. Network Secur.* **8**(2), 138–143 (2008).
19. K. Kim et al., "Real-time foreground-background segmentation using codebook model," *Real-Time Imaging* **11**(3), 172–185 (2005).
20. M. Xiao, C. Han, and X. Kang, "A background reconstruction for dynamic scenes," in *2006 9th Int. Conf. on Information Fusion*, pp. 1–7 (2006).
21. L. Maddalena and A. Petrosino, "A self-organizing approach to background subtraction for visual surveillance applications," *IEEE Trans. Image Process.* **17**(7), 1168–1177 (2008).
22. L. Maddalena and A. Petrosino, "The SOBS algorithm: what are the limits?," in *IEEE Computer Society Conf. on Computer Vision and Pattern Recognition Workshops (CVPRW 2012)*, 21–26 (2012).
23. M. I. Chacon-Murguia and G. Ramirez-Alonso, "Fuzzy-neural self-adapting background modeling with automatic motion analysis for dynamic object detection," *Appl. Soft Comput.* **36**, 570–577 (2015).
24. M. I. Chacon-Murguia et al., "Simplified SOM-neural model for video segmentation of moving object," in *Int. Joint Conf. on Neural Networks*, pp. 474–480 (2009).
25. B. Antic, V. Crnojevic, and D. Culibrk, "Efficient wavelet based detection of moving objects," in *16th Int. Conf. on Digital Signal Processing*, pp. 1–6 (2009).
26. Y.-p. Guan, X.-q. Cheng, and X.-l. Jia, "Motion foreground detection based on wavelet transformation and color ratio difference," in *3rd Int. Congress on Image and Signal Processing (CISP 2010)*, pp. 1423–1426 (2010).
27. S. Messelodi et al., "A Kalman filter based background updating algorithm robust to sharp illumination changes," in *Int. Conf. on Image Analysis and Processing*, pp. 163–170 (2005).
28. A. Morde, X. Ma, and S. Guler, "Learning a background model for change detection," in *IEEE Computer Society Conf. on Computer Vision and Pattern Recognition Workshops (CVPRW 2012)*, pp. 15–20 (2012).
29. G. T. Cinar and J. C. Príncipe, "Adaptive background estimation using an information theoretic cost for hidden state estimation," in *Int. Joint Conf. on Neural Networks (IJCNN 2011)*, pp. 489–494 (2011).
30. N. Goyette et al., "A novel video dataset for change detection benchmarking," *IEEE Trans. Image Process.* **23**(11), 4663–4679 (2014).
31. A. F. Bobick and J. W. Davis, "The recognition of human movement using temporal templates," *IEEE Trans. Pattern Anal. Mach. Intell.* **23**(3), 257–267 (2001).
32. D. Kit, B. Sullivan, and D. Ballard, "Novelty detection using growing neural gas for visuo-spatial memory," in *IEEE/RSJ Int. Conf. on Intelligent Robots and Systems (IROS 2011)*, pp. 1194–1200 (2011).
33. J. Zhong and S. Sclaroff, "Segmenting foreground objects from a dynamic textured background via a robust Kalman filter," in *Proc. Ninth IEEE Int. Conf. on Computer Vision*, pp. 44–50 (2003).
34. F. J. Hernandez-Lopez and M. Rivera, "Change detection by probabilistic segmentation from monocular view," *Mach. Vision Appl.* **25**(5), 1175–1195 (2014).
35. H. Kim et al., "Robust foreground extraction technique using Gaussian family model and multiple thresholds," in *Asian Conf. on Computer Vision 758–768* (2007).
36. F. Porikli and O. Tuzel, "Bayesian background modeling for foreground detection," in *Proc. of the Third ACM Int. Workshop on Video Surveillance & Sensor Networks*, pp. 55–58 (2005).
37. P. Jaikumar, A. Singh, and S. K. Mitra, "Background subtraction in videos using Bayesian learning with motion information," in *British Machine Vision Conf. (BMVC)*, pp. 615–624 (2008).
38. A. Elgammal et al., "Background and foreground modeling using nonparametric kernel density estimation for visual surveillance," *Proc. IEEE* **90**(7), 1151–1163 (2002).
39. O. Barnich and M. Van Droogenbroeck, "ViBe: a universal background subtraction algorithm for video sequences," *IEEE Trans. Image Process.* **20**(6), 1709–1724 (2011).
40. M. Hofmann, P. Tiefenbacher, and G. Rigoll, "Background segmentation with feedback: The pixel-based adaptive segmenter," in *IEEE Computer Society Conf. on Computer Vision and Pattern Recognition Workshops (CVPRW 2012)*, pp. 38–43 (2012).
41. B. Stenger et al., "Topology free hidden Markov models: application to background modeling," in *Proc. Eighth IEEE Int. Conf. on Computer Vision (ICCV 2001)*, pp. 294–301 (2001).
42. N. M. Oliver, B. Rosario, and A. P. Pentland, "A Bayesian computer vision system for modeling human interactions," *IEEE Trans. Pattern Anal. Mach. Intell.* **22**(8), 831–843 (2000).
43. J. Rymel et al., "Adaptive eigen-backgrounds for object detection," in *Int. Conf. on Image Processing (ICIP 2004)*, pp. 1847–1850 (2004).
44. F. Porikli, "Multiplicative background-foreground estimation under uncontrolled illumination using intrinsic images," in *Seventh IEEE Workshops on Application of Computer Vision (WACV/MOTIONS 2005)*, pp. 20–27 (2005).
45. C. Zhao, X. Wang, and W.-K. Cham, "Background subtraction via robust dictionary learning," *EURASIP J. Image Video Process.* **2011**(1), 1–12 (2011).
46. L. Wixson, "Detecting salient motion by accumulating directionally-consistent flow," *IEEE Trans. Pattern Anal. Mach. Intell.* **22**(8), 774–780 (2000).
47. X. Lu and R. Manduchi, "Fast image motion segmentation for surveillance applications," *Image Vision Comput.* **29**(2), 104–116 (2011).
48. D. Zhou and H. Zhang, "Modified GMM background modeling and optical flow for detection of moving objects," in *IEEE Int. Conf. on Systems, Man and Cybernetics*, pp. 2224–2229 (2005).
49. L. Cheng et al., "Real-time discriminative background subtraction," *IEEE Trans. Image Process.* **20**(5), 1401–1414 (2011).
50. B. Han and L. S. Davis, "Density-based multifeature background subtraction with support vector machine," *IEEE Trans. Pattern Anal. Mach. Intell.* **34**(5), 1017–1023 (2012).
51. M. De Gregorio and M. Giordano, "A WiSARD-based approach to CDnet," in *BRICS Congress on Computational Intelligence and 11th Brazilian Congress on Computational Intelligence (BRICS-CCI & CBIC 2013)*, pp. 172–177 (2013).
52. X. Cheng et al., "Improving video foreground segmentation with an object-like pool," *J. Electron. Imaging* **24**(2), 023034 (2015).
53. A. Sobral and A. Vacavant, "A comprehensive review of background subtraction algorithms evaluated with synthetic and real videos," *Comput. Vision Image Understanding* **122**, 4–21 (2014).
54. A. H. Lai and N. H. Yung, "A fast and accurate scoreboard algorithm for estimating stationary backgrounds in an image sequence," in *Proc. of the 1998 IEEE Int. Symp. on Circuits and Systems (ISCAS 1998)*, Vol. 4, pp. 241–244 (1998).

55. N. J. McFarlane and C. P. Schofield, "Segmentation and tracking of piglets in images," *Mach. Vision Appl.* **8**(3), 187–193 (1995).
56. S. Calderara et al., "Reliable background suppression for complex scenes," in *Proc. of the 4th ACM Int. Workshop on Video Surveillance and Sensor Networks*, pp. 211–214 (2006).
57. X. Jian et al., "Background subtraction based on a combination of texture, color and intensity," in *9th Int. Conf. on Signal Processing (ICSP 2008)*, pp. 1400–1405 (2008).
58. P. KaewTraKulPong and R. Bowden, "An improved adaptive background mixture model for real-time tracking with shadow detection," in *Video-Based Surveillance Systems: Computer Vision and Distributed Processing*, P. Remagnino et al., Eds., pp. 135–144, Springer US, Boston, Massachusetts (2002).
59. T. Bouwmans, F. El Baf, and B. Vachon, "Background modeling using mixture of Gaussians for foreground detection-a survey," *Recent Pat. Comput. Sci.* **1**(3), 219–237 (2008).
60. Z. Zivkovic and F. Van Der Heijden, "Efficient adaptive density estimation per image pixel for the task of background subtraction," *Pattern Recognit. Lett.* **27**(7), 773–780 (2006).
61. M. Sivabalan Krishnan and D. Manjula, "Adaptive background subtraction in dynamic environments using fuzzy logic," *Int. J. Comput. Sci. Eng.* **2**(2), 270–273 (2010).
62. T. Bouwmans, "Background subtraction for visual surveillance: a fuzzy approach," *Handb. Soft Comput. Video Surveillance* **5**, 103–138 (2012).
63. Z. Zhao et al., "A fuzzy background modeling approach for motion detection in dynamic backgrounds," in *Multimedia and Signal Processing: Second Int. Conf., CMSPI 2012, Shanghai, China, December 7-9, 2012. Proc.*, F. L. Wang et al., Eds., pp. 177–185, Springer Berlin Heidelberg, Berlin, Heidelberg (2012).
64. D. Culibrk et al., "Neural network approach to background modeling for video object segmentation," *IEEE Trans. Neural Networks* **18**(6), 1614–1627 (2007).
65. L. Maddalena and A. Petrosino, "A fuzzy spatial coherence-based approach to background/foreground separation for moving object detection," *Neural Comput. Appl.* **19**(2), 179–186 (2010).
66. Y. Goya et al., "Vehicle trajectories evaluation by static video sensors," in *IEEE Intelligent Transportation Systems Conf. (ITSC 2006)*, pp. 864–869 (2006).
67. K. Sehairi, F. Chouireb, and J. Meunier, "Comparison study between different automatic threshold algorithms for motion detection," in *4th Int. Conf. on Electrical Engineering (ICEE 2015)*, pp. 1–8 (2015).
68. M. Van Droogenbroeck and O. Paquot, "Background subtraction: experiments and improvements for ViBe," in *IEEE Computer Society Conf. on Computer Vision and Pattern Recognition Workshops (CVPRW 2012)*, pp. 32–37 (2012).
69. T. Bouwmans and E. H. Zahzah, "Robust PCA via principal component pursuit: a review for a comparative evaluation in video surveillance," *Comput. Vision Image Understanding* **122**, 22–34 (2014).
70. T. Bouwmans et al., "Decomposition into low-rank plus additive matrices for background/foreground separation: a review for a comparative evaluation with a large-scale dataset," *Comput. Sci. Rev.* **23**, 1–71 (2017).
71. R. Cabral et al., "Unifying nuclear norm and bilinear factorization approaches for low-rank matrix decomposition," in *Proc. of the IEEE Int. Conf. on Computer Vision*, pp. 2488–2495 (2013).
72. N. Wang and D.-Y. Yeung, "Bayesian robust matrix factorization for image and video processing," in *Proc. of the IEEE Int. Conf. on Computer Vision*, pp. 1785–1792 (2013).
73. C. Guyon, T. Bouwmans, and E.-H. Zahzah, "Foreground detection via robust low rank matrix factorization including spatial constraint with iterative reweighted regression," in *21st Int. Conf. on Pattern Recognition (ICPR 2012)*, pp. 2805–2808 (2012).
74. S. Javed et al., "Robust background subtraction to global illumination changes via multiple features-based online robust principal components analysis with Markov random field," *J. Electron. Imaging* **24**(4), 043011 (2015).
75. B. Zhou, F. Zhang, and L. Peng, "Background modeling for dynamic scenes using tensor decomposition," in *6th Int. Conf. on Electronics Information and Emergency Communication (ICEIEC 2016)*, pp. 206–210 (2016).
76. W. Cao et al., "Total variation regularized tensor RPCA for background subtraction from compressive measurements," *IEEE Trans. Image Process.* **25**(9), 4075–4090 (2016).
77. A. Sobral et al., "Online stochastic tensor decomposition for background subtraction in multispectral video sequences," in *Proc. of the IEEE Int. Conf. on Computer Vision Workshops*, pp. 106–113 (2015).
78. T. Bouwmans, "Traditional and recent approaches in background modeling for foreground detection: an overview," *Comput. Sci. Rev.* **11**, 31–66 (2014).
79. S. Y. Elhabian, K. M. El-Sayed, and S. H. Ahmed, "Moving object detection in spatial domain using background removal techniques-state-of-art," *Recent Pat. Comput. Sci.* **1**(1), 32–54 (2008).
80. G. Morris and P. Angelov, "Real-time novelty detection in video using background subtraction techniques: state of the art a practical review," in *IEEE Int. Conf. on Systems, Man and Cybernetics (SMC 2014)*, pp. 537–543 (2014).
81. T. Bouwmans, "Subspace learning for background modeling: a survey," *Recent Pat. Comput. Sci.* **2**(3), 223–234 (2009).
82. C. Cuevas, R. Martinez, and N. Garcia, "Detection of stationary foreground objects: a survey," *Comput. Vision Image Understanding* **152**, 41–57 (2016).
83. A. Bux, P. Angelov, and Z. Habib, "Vision based human activity recognition: a review," in *Advances in Computational Intelligence Systems: Contributions Presented at the 16th UK Workshop on Computational Intelligence, September 7–9, 2016, Lancaster, UK*, P. Angelov et al., Eds., pp. 341–371, Springer International Publishing, Cham (2017).
84. M. Cristani et al., "Background subtraction for automated multisensor surveillance: a comprehensive review," *EURASIP J. Adv. Signal Process.* **2010**(1), 343057 (2010).
85. <http://research.microsoft.com/en-us/um/people/jckrumm/wallflower/testimages.htm>.
86. K. Toyama et al., "Wallflower: principles and practice of background maintenance," in *the Proc. of the Seventh IEEE Int. Conf. on Computer Vision*, pp. 255–261 (1999).
87. T. Matsuyama, T. Ohya, and H. Habé, "Background subtraction for non-stationary scenes," in *Proc. of Asian Conf. on Computer Vision*, pp. 662–667 (2000).
88. I. Haritaoglu, D. Harwood, and L. S. Davis, "W4S: a real-time system for detecting and tracking people in 2 1/2D," in *European Conf. on Computer Vision*, pp. 877–892 (1998).
89. H. Nakai, "Non-parameterized Bayes decision method for moving object detection," in *Proc. Asian Conference on Computer Vision (ACCV)*, pp. 447–451 (1995).
90. B. Lo and S. Velastin, "Automatic congestion detection system for underground platforms," in *Proc. of 2001 Int. Symp. on Intelligent Multimedia, Video, and Speech Processing*, pp. 158–161 (2001).
91. R. Cucchiara et al., "Detecting moving objects, ghosts, and shadows in video streams," *IEEE Trans. Pattern Anal. Mach. Intell.* **25**(10), 1337–1342 (2003).
92. B. Han, D. Comaniciu, and L. Davis, "Sequential kernel density approximation through mode propagation: applications to background modeling," in *Asian Conf. on Computer Vision (ACCV 2004)*, pp. 818–823 (2004).
93. M. Seki et al., "Background subtraction based on cooccurrence of image variations," in *Proc. IEEE Computer Society Conf. on Computer Vision and Pattern Recognition*, pp. 65–72 (2003).
94. S.-C. S. Cheung and C. Kamath, "Robust background subtraction with foreground validation for urban traffic video," *EURASIP J. Adv. Signal Process.* **2005**(14), 726261 (2005).
95. K. Karmann and A. Brandt, "Moving object recognition using and adaptive background memory," in *Time-Varying Image Processing and Moving Object Recognition*, V. Cappellini, Ed., Vol. 2, pp. 289–307 (1990).
96. http://i21www.ira.uka.de/image_sequences/.
97. Y. Benezech et al., "Comparative study of background subtraction algorithms," *J. Electron. Imaging* **19**(3), 033003 (2010).
98. <http://imagelab.ing.unimore.it/vssn06/>.
99. L. M. Brown et al., "Performance evaluation of surveillance systems under varying conditions," in *Proc. IEEE PETS Workshop*, pp. 1–8 (2005).
100. B. White and M. Shah, "Automatically tuning background subtraction parameters using particle swarm optimization," in *IEEE Int. Conf. on Multimedia and Expo*, pp. 1826–1829 (2007).
101. Hanzi W. and D. Suter, "A re-evaluation of mixture of Gaussian background modeling [video signal processing applications]," in *Proc. IEEE Int. Conf. on Acoustics, Speech, and Signal Processing (ICASSP 2005)*, Vol. **1012** pp. ii/1017–ii/1020 (2005).
102. K. Schindler and H. Wang, "Smooth foreground-background segmentation for video processing," in *Asian Conf. on Computer Vision*, pp. 581–590 (2006).
103. N. A. Setiawan et al., "Gaussian mixture model in improved HLS color space for human silhouette extraction," in *Advances in Artificial Reality and Tele-Existence*, pp. 732–741, Springer (2006).
104. M. Cristani and V. Murino, "A spatial sampling mechanism for effective background subtraction," in *Proc. 2nd Int. Conf. on Computer Vision Theory and Applications (VISAPP 2007)*, pp. 403–412 (2007).
105. M. Cristani and V. Murino, "Background subtraction with adaptive spatio-temporal neighborhood analysis," in *Proc. 2nd Int. Conf. on Computer Vision Theory and Applications (VISAPP 2007)*, pp. 484–489 (2008).
106. D.-M. Tsai and S.-C. Lai, "Independent component analysis-based background subtraction for indoor surveillance," *IEEE Trans. Image Process.* **18**(1), 158–167 (2009).
107. S. S. Bucak, B. Günsel, and O. Gursoy, "Incremental non-negative matrix factorization for dynamic background modelling," in *Pattern Recognition in Information Systems (PRIS)*, pp. 107–116 (2007).
108. X. Li et al., "Robust foreground segmentation based on two effective background models," in *Proc. of the 1st ACM Int. Conf. on Multimedia Information Retrieval*, pp. 223–228 (2008).
109. N. Goyette et al., "Changedetection.net: a new change detection benchmark dataset," in *IEEE Computer Society Conf. on Computer*

- Vision and Pattern Recognition Workshops (CVPRW 2012)*, pp. 1–8 (2012).
110. J.-P. Jodoin, G.-A. Bilodeau, and N. Saunier, “Background subtraction based on local shape,” arXiv preprint arXiv:1204.6326 (2012).
 111. D. Riahi, P. St-Onge, and G. Bilodeau, “RECTGAUSS-tex: block-based background subtraction,” in *Proce Dept. genie Inform. genie logiciel, Ecole Polytechn. Montr. QC, Canada*, pp. 1–9 (2012).
 112. Y. Nonaka et al., “Evaluation report of integrated background modeling based on spatio-temporal features,” in *IEEE Computer Society Conf. on Computer Vision and Pattern Recognition Workshops (CVPRW 2012)*, pp. 9–14 (2012).
 113. S. Yoshinaga et al., “Background model based on intensity change similarity among pixels,” in *19th Korea-Japan Joint Workshop on Frontiers of Computer Vision (FCV 2013)*, pp. 276–280 (2013).
 114. A. Schick, M. Bäuml, and R. Stiefelhagen, “Improving foreground segmentations with probabilistic superpixel markov random fields,” in *IEEE Workshop on Change Detection* (2012).
 115. <http://wordpress-jodoin.dmi.usherba.ca/dataset2012/>.
 116. Y. Wang et al., “CDnet 2014: an expanded change detection benchmark dataset,” in *Proc. of the IEEE Conf. on Computer Vision and Pattern Recognition Workshops*, pp. 387–394 (2014).
 117. X. Lu, “A multiscale spatio-temporal background model for motion detection,” in *IEEE Int. Conf. on Image Processing (ICIP 2014)*, pp. 3268–3271 (2014).
 118. D. Liang and S. i. Kaneko, “Improvements and experiments of a compact statistical background model,” arXiv preprint arXiv:1405.6275 (2014).
 119. B. Tamás, “Detecting and analyzing rowing motion in videos,” in *BME Scientific Student Conf.*, Budapest, pp. 1–29 (2016).
 120. B. Wang and P. Dudek, “A fast self-tuning background subtraction algorithm,” in *Proc. of the IEEE Conf. on Computer Vision and Pattern Recognition Workshops*, pp. 395–398 (2014).
 121. M. Sedky, M. Moniri, and C. C. Chibelushi, “Spectral-360: a physics-based technique for change detection,” in *Proc. of the IEEE Conf. on Computer Vision and Pattern Recognition Workshops*, pp. 399–402 (2014).
 122. M. De Gregorio and M. Giordano, “Change detection with weightless neural networks,” in *Proc. of the IEEE Conf. on Computer Vision and Pattern Recognition Workshops*, pp. 403–407 (2014).
 123. P.-L. St-Charles, G.-A. Bilodeau, and R. Bergevin, “Flexible background subtraction with self-balanced local sensitivity,” in *Proc. of the IEEE Conf. on Computer Vision and Pattern Recognition Workshops*, pp. 408–413 (2014).
 124. R. Wang et al., “Static and moving object detection using flux tensor with split Gaussian models,” *Proc. of the IEEE Conf. on Computer Vision and Pattern Recognition Workshops*, pp. 414–418 (2014).
 125. P.-M. Jodoin et al., “Overview and benchmarking of motion detection methods,” in *Background Modeling and Foreground Detection for Video Surveillance*, T. Bouwmans et al., Eds., CRC Press, Boca Raton, Florida (2014).
 126. R. H. Evangelio and T. Sikora, “Complementary background models for the detection of static and moving objects in crowded environments,” in *8th IEEE Int. Conf. on Advanced Video and Signal-Based Surveillance (AVSS 2011)*, pp. 71–76 (2011).
 127. R. H. Evangelio, M. Pätzold, and T. Sikora, “Splitting Gaussians in mixture models,” in *IEEE Ninth Int. Conf. on Advanced Video and Signal-Based Surveillance (AVSS 2012)*, pp. 300–305 (2012).
 128. T. S. Haines and T. Xiang, “Background subtraction with dirichlet processes,” in *European Conf. on Computer Vision*, pp. 99–113 (2012).
 129. S. Bianco, G. Ciocca, and R. Schettini, “How far can you get by combining change detection algorithms?,” arXiv preprint arXiv:1505.02921 (2015).
 130. S. Varadarajan, P. Miller, and H. Zhou, “Spatial mixture of Gaussians for dynamic background modelling,” in *10th IEEE Int. Conf. on Advanced Video and Signal Based Surveillance (AVSS 2013)*, pp. 63–68 (2013).
 131. <http://wordpress-jodoin.dmi.usherba.ca/dataset2014/>.
 132. Y. Xu et al., “Background modeling methods in video analysis: a review and comparative evaluation,” *CAAI Trans. Intell. Technol.* **1**(1), 43–60 (2016).
 133. H. Wang and D. Suter, “A consensus-based method for tracking: modelling background scenario and foreground appearance,” *Pattern Recognit.* **40**(3), 1091–1105 (2007).
 134. H. Wang and D. Suter, “Background subtraction based on a robust consensus method,” in *18th Int. Conf. on Pattern Recognition (ICPR 2006)*, pp. 223–226 (2006).
 135. J. Wen et al., “Joint video frame set division and low-rank decomposition for background subtraction,” *IEEE Trans. Circuits Syst. Video Technol.* **24**(12), 2034–2048 (2014).
 136. Y. Sheikh and M. Shah, “Bayesian modeling of dynamic scenes for object detection,” *IEEE Trans. Pattern Anal. Mach. Intell.* **27**(11), 1778–1792 (2005). <http://www.cs.cmu.edu/~yaser/#software>.
 137. V. Mahadevan and N. Vasconcelos, “Spatiotemporal saliency in dynamic scenes,” *IEEE Trans. Pattern Anal. Mach. Intell.* **32**(1), 171–177 (2010). http://www.svcl.ucsd.edu/projects/background_subtraction/ucsdbsub_dataset.htm.
 138. A. Vacavant et al., “A benchmark dataset for outdoor foreground/background extraction,” in *Asian Conf. on Computer Vision*, pp. 291–300 (2012). <http://bmc.iut-auvergne.com/>.
 139. A. Doulamis et al., “An architecture for a self configurable video supervision,” in *Proc. of the 1st ACM Workshop on Analysis and Retrieval of Events/Actions and Workflows in Video streams*, pp. 97–104 (2008).
 140. D. D. Bloisi et al., “ARGOS-Venice boat classification,” in *12th IEEE Int. Conf. on Advanced Video and Signal Based Surveillance (AVSS 2015)*, pp. 1–6 (2015). <http://www.dis.uniroma1.it/~labrococo/MAR/index.htm>.
 141. J. Gallego Vila, “Parametric region-based foreround segmentation in planar and multi-view sequences” (2013). <https://image.upc.edu/web/resources/kinect-database-foreground-segmentation>.
 142. M. Camplani and L. Salgado, “Background foreground segmentation with RGB-D Kinect data: an efficient combination of classifiers,” *J. Visual Commun. Image Represent.* **25**(1), 122–136 (2014). <http://eis.bristol.ac.uk/~mc13306/>.
 143. B. J. Boom et al., “A research tool for long-term and continuous analysis of fish assemblage in coral-reefs using underwater camera footage,” *Ecol. Inf.* **23**, 83–97 (2014). <http://groups.inf.ed.ac.uk/f4k/index.html>.
 144. S. K. Choudhury et al., “An evaluation of background subtraction for object detection vis-a-vis mitigating challenging scenarios,” *IEEE Access* **4**, 6133–6150 (2016).
 145. D. H. Parks and S. S. Fels, “Evaluation of background subtraction algorithms with post-processing,” in *IEEE Fifth Int. Conf. on Advanced Video and Signal Based Surveillance (AVSS 2008)*, pp. 192–199 (2008).
 146. S. Joudaki, M. S. B. Sunar, and H. Kolivand, “Background subtraction methods in video streams: a review,” in *4th Int. Conf. on Interactive Digital Media (ICIDM 2015)*, pp. 1–6 (2015).
 147. Y. Dhome et al., “A benchmark for background subtraction algorithms in monocular vision: a comparative study,” in *2nd Int. Conf. on Image Processing Theory Tools and Applications (IPTA 2010)*, pp. 66–71 (2010).
 148. D. K. Prasad et al., “Video processing from electro-optical sensors for object detection and tracking in maritime environment: a survey,” in *IEEE Transactions on Intelligent Transportation Systems*, pp. 1–24 (2017).
 149. Z. Wang, J. Xiong, and Q. Zhang, “Motion saliency detection based on temporal difference,” *J. Electron. Imaging* **24**(3), 033022 (2015).
 150. S. S. M. Radzi et al., “Extraction of moving objects using frame differencing, ghost and shadow removal,” in *5th Int. Conf. on Intelligent Systems, Modelling and Simulation (ISMS 2014)*, pp. 229–234 (2014).
 151. C. Chen and X. Zhang, “Moving vehicle detection based on union of three-frame difference,” in *Advances in Electronic Engineering, Communication and Management Vol.2: Proceedings of 2011 International Conference on Electronic Engineering, Communication and Management (EECM 2011), held on December 24–25, 2011, Beijing, China*, D. Jin and Lin S., Eds., pp. 459–464, Springer Berlin Heidelberg, Berlin, Heidelberg (2012).
 152. Z. Wang, “Hardware implementation for a hand recognition system on FPGA,” in *5th Int. Conf. on Electronics Information and Emergency Communication (ICEIEC 2015)*, pp. 34–38 (2015).
 153. Y. Zhang, X. Wang, and B. Qu, “Three-frame difference algorithm research based on mathematical morphology,” *Proc. Eng.* **29**, 2705–2709 (2012).
 154. J. Heikkilä and O. Silvén, “A real-time system for monitoring of cyclists and pedestrians,” *Image Vision Comput.* **22**(7), 563–570 (2004).
 155. X.-j. Tan, J. Li, and C. Liu, “A video-based real-time vehicle detection method by classified background learning,” *World Trans. Eng. Technol. Edu.* **6**(1), 189 (2007).
 156. J. Richefeu and A. Manzanera, “A new hybrid differential filter for motion detection,” in *Computer Vision and Graphics: Int. Conf., ICCVG 2004, Warsaw, Poland, September 2004, Proc.*, K. Wojciechowski et al., Eds., pp. 727–732, Springer, Netherlands, Dordrecht (2006).
 157. A. Manzanera and J. C. Richefeu, “A new motion detection algorithm based on $\Sigma - \Delta$ background estimation,” *Pattern Recognit. Lett.* **28**(3), 320–328 (2007).
 158. L. Lacassagne et al., “High performance motion detection: some trends toward new embedded architectures for vision systems,” *J. Real-Time Image Process.* **4**(2), 127–146 (2009).
 159. P. Bouthemy and P. Lalonde, “Recovery of moving object masks in an image sequence using local spatiotemporal contextual information,” *Opt. Eng.* **32**(6), 1205–1212 (1993).
 160. A. Caplier, F. Luthon, and C. Dumontier, “Real-time implementations of an MRF-based motion detection algorithm,” *Real-Time Imaging* **4**(1), 41–54 (1998).
 161. J. Denoulet et al., “Implementing motion Markov detection on general purpose processor and associative mesh,” in *Proc. Seventh Int. Workshop on Computer Architecture for Machine Perception (CAMP 2005)*, pp. 288–293 (2005).